First-order magnetic-field-induced phase transition in epitaxial iron films studied by magnetoresistance

K. T. Riggs* and E. Dan Dahlberg
School of Physics and Astronomy, University of Minnesota, Minneapolis, Minnesota 55455

G. A. Prinz
Naval Research Laboratory, Washington, D.C. 20375-5000
(Received 31 August 1989)

The magnetic-field-driven magnetization-reorientation phase transition in epitaxially grown Fe/GaAs(110) thin films (thickness 9–20 nm), first reported by Hathaway and Prinz, has been studied using anisotropic magnetoresistance (AMR) as a probe of the direction of magnetization. In AMR measurements, just as in ferromagnetic resonance (FMR), the ratios of the anisotropy constants to the magnetization are determined. In the present work the iron film thickness dependence of the ratios of the fourth-order (K_1) and uniaxial (K_u) anisotropy constants to the magnetization were found comparable with previous FMR results. In addition, using values of the thickness dependence of the saturation magnetization, the present work includes the thickness dependence of K_1 and K_u. The observed thickness dependence of K_1 is similar to that seen previously in Ni/NaCl systems and may be due to strain-induced magnetostriction effects. Considerable hysteresis at the magnetization-reorientation transition is observed. The magnitude of the hysteresis is considerably less than that calculated from the anisotropy energies for uniform rotation of the magnetization. It is therefore reasonable to assume that the magnetization process occurs by domain-wall nucleation and propagation and that the hysteresis is associated with domain-wall pinning.

I. INTRODUCTION

The recent application of molecular beam epitaxy (MBE) to the study of magnetism has resulted in an explosion of interest in the possibility of engineering magnetic properties on an atomic scale.[1] Novel magnetic properties not present in corresponding bulk magnetic systems have been widely reported. Magnetic moments, exchange interactions, and magnetic anisotropies are all predicted to vary as the local environment of the magnetic species is changed.[2–5] This fact opens up a whole new area of fundamental study in magnetism, as well as great technological promise.[6,7]

Two examples of the novel behavior mentioned above are a uniaxial magnetic anisotropy and a first-order magnetization-reorientation phase transition (MRPT) (Refs. 8–11) induced by an applied magnetic field, both of which have been observed in the epitaxial Fe(110)/GaAs system.[12] A first-order MRPT is predicted in bulk Fe for applied fields near the ⟨111⟩ direction.[13,14] While this transition has been observed in other cubic ferromagnets,[15,16] it has been long sought but never observed in bulk Fe single crystals.[17,18]

Two factors change the situation in Fe/GaAs thin films. First, the large demagnetizing field normal to the film plane due to the shape anisotropy forces the magnetization to lie in the plane of the film [no evidence of a large uniaxial anisotropy perpendicular to the plane has been found in the Fe/GaAs system[19] unlike that predicted for the Fe(100)/Ag system].[4] This fact alone considerably modifies the bulk Fe MRPT phase diagram and allows the transition to be observed for a wide range of angles about the ⟨110⟩ direction. The predicted first-order discontinuity in the magnetization direction is also increased by a large factor, enabling the experimental detection of the transition with greater ease.

Second, the uniaxial anisotropy, first proposed by Prinz *et al.*[11] in order to explain ferromagnetic resonance (FMR) data, further modifies the MRPT phase diagram in a well-defined way. The dependence of the MRPT phase diagram on the ratios of the relevant anisotropy constants to the magnetization enables one to extract the ratios from an experimental determination of the first-order transition boundary as a function of applied magnetic field.

We have undertaken a systematic study of the first-order MRPT in five Fe(110)/GaAs films (thickness 9–20 nm) using anisotropic magnetoresistance (AMR) (Ref. 20) as a probe of the direction of magnetization. The advantages of using AMR over the more conventional methods of FMR and vibrating sample magnetometry (VSM) are the ease of the resistance measurement and the technique's lack of sensitivity to the magnetic properties of the nonmetallic substrate.[21]

This paper will focus on a method to extract the important anisotropy constants from the experimental MRPT phase diagrams. The results for K_u/M_s and K_1/M_s are found to be in qualitative agreement with the FMR results of Prinz *et al.* on similar films.[10] We will also present an interpretation of the hysteresis observed at the first-order transition. Our data support the conjecture that domain-wall pinning[10,22,23] and not transitions

 ©1990 The American Physical Society

out of a metastable state due to fluctuations[24] is the likely explanation for the observed width of the hysteresis.

II. SAMPLE DESCRIPTION

The epitaxial Fe(110) films are deposited on polished, chemically etched and ultrahigh-vacuum (UHV) thermally annealed GaAs(110) substrates. Thickness is determined by monitoring the Fe flux with a quadrupole mass spectrometer calibrated via x-ray fluorescence measurements on thicker films. The epitaxial growth of the iron films is monitored by *in situ* reflection high-energy electron diffraction (RHEED) and it is found that the 1.4% lattice mismatch between the GaAs lattice constant and twice the Fe lattice constant results in a compression of the Fe lattice at the Fe/GaAs interface. RHEED data suggests that this strain relaxes, presumably by introducing point defects or dislocations; at a thickness of about 20 nm the iron lattice constant is that of bulk iron.

The films were allowed to oxidize after removal from the UHV environment. A surface oxide layer of approximately 3 nm is formed removing about 1.5 nm of Fe from the nominal thickness.[25] In what follows, only the preoxidation nominal thickness is reported. This oxide layer is self-passivating, inhibiting further oxidation. The oxide layer is remarkably stable and the measured resistivities of the films have remained constant over a period of several years and repeated thermal cycling.

The samples were patterned with photolithographic techniques with Hall bar geometries enabling transport measurements along three high symmetry directions contained in the (110) plane. The AMR measurements reported here were performed with the current, **J**, in the [110] direction, except for the thickest film (20 nm) where the current was in the [001] direction. We should note that results for the thinner films, where both current directions were used, show that the MRPT phase diagram is independent of current direction.

III. EXPERIMENTAL DETAILS

A simple technique to gain information on the state of magnetization of a ferromagnetic thin film sample on a nonconducting substrate is to utilize the fact that the diagonal or longitudinal resistivity depends on the orientation of the magnetization with respect to the direction of the current. This effect, called the anisotropic magnetoresistance (AMR), has a long and interesting history beginning with its discovery in 1857 by William Thompson (Lord Kelvin).[20] This effect arises in $3d$ ferromagnetic transition metals due to spin orbit coupling and d band splitting.[26]

To lowest order, the resistivity depends on the angle (β) the magnetization vector makes with respect to the current direction as

$$\rho(\theta)=\rho_T+\Delta\rho\cos^2\beta\ , \tag{1}$$

where $\Delta\rho=\rho_L-\rho_T$ and (L) indicates longitudinal (**M** parallel to current) and (T) indicates transverse (**M** perpendicular to current) resistivities, respectively. The angular dependence of Eq. (1) has been confirmed experimentally in our films;[21] a detailed analysis of $\Delta\rho/\rho$ for these films will be presented elsewhere.[27] In practice by measuring the deviations from the predicted dependence of the applied magnetic field and the current one can determine the anisotropy energies. These deviations occur when the magnetic energy $\mathbf{M}\cdot\mathbf{H}$ becomes comparable to the anisotropy energies. For the films reported here the situation is even simpler since in the plane of the film a hard direction (the [111]) separates the easy axis (the [100]) from the intermediate direction (the [110]). The details of how this simplifies the situation are in the next section.

Before proceeding to the next section, a few additional comments are necessary. Since the resistivity is an even function of θ, there is ambiguity as to the sign of **M**. However, in what follows we always saturate the sample along the "easy" [001] direction before each field sweep. This allows the sample to be left in a known initial state. Magnetization studies[8] have shown that the hysteresis loop is nearly square in the [001] direction indicating that we are always beginning with a nearly monodomain sample with the magnetization along this "easy" [001] direction. Also, since the AMR effect is quite small in Fe ($\Delta\rho/\rho\simeq 0.2\%$) a high sensitivity method to measure the change in resistance is required. We have used an ac resistance bridge technique with a typical excitation current of 20 μA.

IV. THE MAGNETIZATION REORIENTATION PHASE TRANSITION (MRPT) PHASE DIAGRAM

The MRPT phase diagram can be theoretically calculated by considering the usual phenomenological expansion of the energy density in terms of anisotropy constants appropriate to a material like Fe with cubic symmetry. The energy density of a single domain with magnetization **M** in an applied field **H** can be written

$$E=-\mathbf{H}\cdot\mathbf{M}+2\pi M_n^2+K_u\sin^2\gamma+K_u'\sin^4\gamma+K_n(M_n/M)^2 +K_1(\alpha_1^2\alpha_2^2+\alpha_2^2\alpha_3^2+\alpha_3^2\alpha_1^2)+K_2(\alpha_1^2\alpha_2^2\alpha_3^2)+\cdots\ , \tag{2}$$

where $\hat{\boldsymbol{\alpha}}=\mathbf{M}/M$ is the magnetization direction relative to the cubic crystalline axes, M_n is the component of the magnetization normal to the film plane, and γ is measured in the plane of the film relative to the [001] axis.

There is evidence that the anisotropy term K_n is very small for the Fe(110) surface[19] unlike the situation for Fe(100) on silver[5] where K_n can dominate the shape anisotropy term. For the Fe(110) case we will neglect K_n compared to $2\pi M^2$. Thus, the shape anisotropy term, $2\pi M_n^2$, corresponding to a thin film, forces the magnetization to reside in the film plane for $H_n=0$ and $K_1\ll 2\pi M^2$. Since $K_1/M\simeq 275$ Oe and $4\pi M\simeq 20$ kOe for bulk Fe it is clear that this approximation is well justified. The terms containing the constants K_u and K_u' are uniaxial terms introduced by Prinz *et al.*[9] in order to fit FMR data on similar Fe(110)/GaAs films. The in-plane uniaxial terms can occur due to the reduced symmetry of the Fe/GaAs and Fe/Fe oxide interfacial lay-

ers[28] and could be due to strain-induced magnetostriction.

The terms containing K_1 and K_2 are the usual anisotropy constants appropriate to a material with cubic symmetry.[29] Since in bulk Fe K_1 is more than two orders of magnitude larger than K_2 at room temperature[30] it is safe for our purposes to neglect K_2 and all higher order terms in the expansion. This leaves K_1, K_u, and K_u' as the adjustable parameters. In fitting, it was determined that the only adjustable constants required to explain the observed data are K_1 and K_u.

For the purpose of calculation it is convenient to measure the direction of the magnetization relative to the [110] direction (angle θ) and to define a reduced energy density $\epsilon = E/K_1$ and reduced field $h = H/(K_1/M)$ as well as the ratio $\kappa = K_u/K_1$.[14] Then for the magnetization confined to the plane of the film the reduced energy density becomes

$$\epsilon(\theta) = -h\cos(\theta-\theta_H) + \tfrac{1}{2}(1-\sin^4\theta-\tfrac{1}{2}\cos^4\theta)-\kappa\sin^2\theta\ , \quad (3)$$

where θ is the angle of the in-plane applied field with respect to the [110] direction and θ_H is the angle of the applied magnetic field again measured from the [110]. In zero field, when $K_1 > 0$ and $\kappa > -\frac{1}{4}$, the easy axis is the [001] direction with the [111] axis as the hard direction and the [110] axis as the intermediate direction. When $\kappa \le -\frac{1}{4}$ the [001] direction becomes the easy axis. A pronounced dependence of κ with thickness has been observed[9,11] resulting in a switching of the easy axis from [001] for thicknesses greater than about 10 nm to [110] for thicknesses less than about 10 nm. The precise thickness at which the easy axis switches is somewhat sensitive to the conditions of epitaxial growth. We have observed the same qualitative thickness dependence in this work.

For all of the films discussed here, the easy direction for the magnetization is a [100] direction. For these films, an applied magnetic field in the [110] direction ($\theta_H = 0$) will rotate the magnetization smoothly away from the easy direction with the magnitude of the rotation determined by the anisotropy energy along the hard or [111] direction. At some "critical" reduced field, $h_p(\kappa)$, the magnetization jumps discontinuously into alignment with the applied field. In theory this jump occurs when the two states, the one just before the jump and the one with the magnetization parallel to the [110], become energetically degenerate. In practice the transition is observed to be hysteretic since to jump from one state to the other involves overcoming an energy barrier. An example of this first-order jump for a typical sample is shown in Fig. 1. The two crosses in the figure mark the location and magnitude of the predicted discontinuity in the resistance using the K_1, K_u obtained from the experimental MRPT phase diagram. Note that there is considerable hysteresis at the transition. This hysteresis is completely reproducible from run to run and does not depend on the field sweep rate. The likely cause of this hysteresis is one of the questions we would like to consider in what follows.

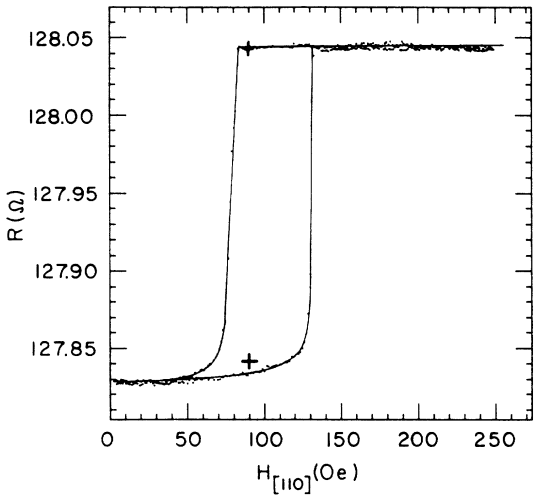

FIG. 1. The resistive transition in a 16.0-nm-thick film with the magnetic applied in the plane of the film parallel to the [110] direction. This figure exhibits the hysteresis which is observed with increasing and decreasing magnetic field. The + data points mark the expected position and magnitude of the transition calculated from the fitted experimental anisotropy constants.

For fields rotated away from the [110] direction, a similar first-order discontinuity occurs but is shifted to higher values of the reduced field. At some critical angle θ_{Hc} and reduced field h_c the transition becomes second order and the discontinuity in magnetization direction vanishes. This point is analogous to the critical end point (CEP) for a gas described by the van der Waals equation of state. Calculating where the transition occurs for angles between $\theta_H = 0$ and $\theta_H = \theta_{Hc}$ becomes analytically intractable. We have instead numerically solved the system of nonlinear equations to map out the phase diagram in this region. It turns out that phase boundary is very nearly a straight line connecting h_p and the critical end point for all values of κ. The results of this numerical calculation, including the relevant parameters corresponding to the MRPT phase diagram, are shown in Fig. 2.

The quantities θ_{Hc}, h_c, and h_p are all functions of the ratio $\kappa = K_u/K_1$ only, and can be calculated analytically by analyzing the behavior of Eq. (3). This can be accomplished by looking for the point where the two minima of the function become equal in energy in the case of h_p and where the two minima become degenerate in the case of θ_{Hc} and h_c. The results of this calculation are as follows. The critical angle θ_{Hc} is given by the relation

$$\tan\theta_{Hc} = [(7-2\kappa)/(2\kappa+8)]^{5/2}\ , \quad (4)$$

and the reduced magnetic field at the critical end point h_c is given by

$$h_c = \sin\phi\cos\phi(2\sin^2\phi-\cos^2\phi+2\kappa)/\sin(\phi-\theta_{Hc})\ , \quad (5)$$

where ϕ is the angle the magnetization makes relative to the [110] axis at the critical end point. In terms of κ this

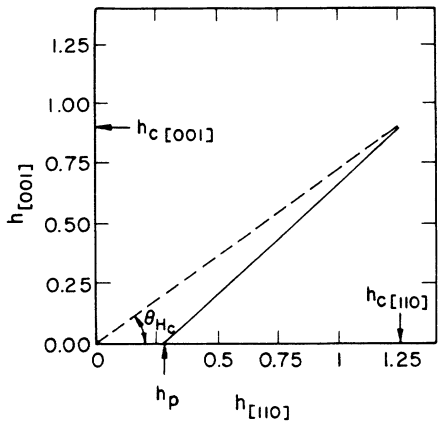

FIG. 2. The calculated phase diagram for the first-order transition of the magnetization. The phase boundary is terminated by a critical end point (CEP) when the magnetic field is applied located nearly parallel to the hard [111] direction. The other notation is explained in the text.

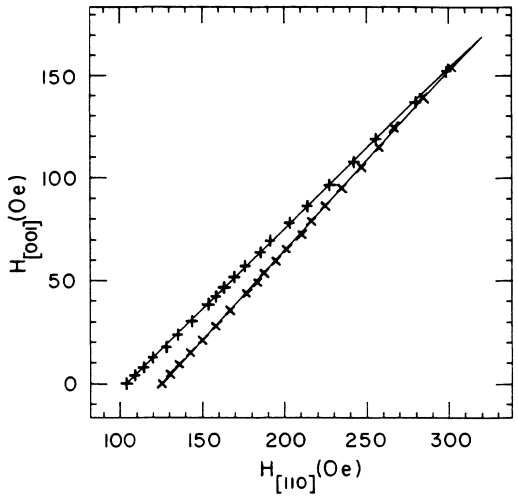

FIG. 3. The experimental phase diagram for a 17.2-nm film. The × points indicate increasing field and the + points indicate decreasing field. The fact that the hysteresis must vanish at the critical end point is used to determine its position.

angle can be found from the relation

$$\sin\phi=[(21-6\kappa)/45]^{1/2} . \tag{6}$$

The reduced field for $\theta_{Hc}=0$ can be determined by the expression

$$h_p=(1-\eta^2)^{1/2}(3\eta^2+2\kappa-1) , \tag{7}$$

with η being the normalized component of the magnetization parallel to the [001] easy direction ($\eta=M_{[001]}/M$) just below the reduced field $h=h_p$. This quantity plays a role somewhat analogous to the order parameter in a standard thermal phase transition and is given by the equation

$$\eta^2=\tfrac{2}{9}[(3-2\kappa)+(2+4\kappa)^{1/2}] . \tag{8}$$

The above results are only valid for κ within the range $-\frac{1}{4}\leq\kappa\leq\frac{7}{2}$. When $\kappa<-\frac{1}{4}$ (assuming K_1 remains positive), the easy axis switches to the [110] direction and no first-order magnetization-reorientation transitions are possible. For $\kappa>\frac{7}{2}$ the critical end point falls along the [110] direction ($\theta_{Hc}=0$) and again no first-order transitions can occur.

V. DISCUSSION

A. Anisotropy energies

The anisotropy constants $K_1/M, K_u/M$ can be extracted from the experimental phase diagrams and the above expressions in the following manner. We first determine θ_{Hc} from the experimental phase diagram by noting where the hysteresis associated with the MRPT vanishes. This is assumed to occur at the point where the transition becomes second order. Operationally, this is accomplished by fitting the field sweep up and down transition points with a low order polynomial (normally linear) and extrapolating to the intersection of the two functions. An example of this procedure is shown in Fig. 3. Once an experimental value for θ_{Hc} is determined, Eq. (4) can be inverted to yield the value of κ for each film. From the experimental field at the critical end point, H_c(expt), and the theoretical value from Eq. (5), the ratio

$$K_1/M=H_c(\text{expt})h_c \tag{9}$$

can be determined.

A self-consistent check of the results of this analysis to determine κ can be performed by calculating the predicted field where the jump is expected along the [110] direction,

$$H_p(\kappa)=h_p(\kappa)(K_1/M) . \tag{10}$$

This result can be compared with the experimental phase diagram. Of the five films studied, the field calculated via Eq (10) fell between the hysteretic transitions points in all but the 13.7 nm film, as one might expect. However, no consistent pattern of exactly where this point falls relative to the experimental hysteresis points was found. The field predicted by Eq. (10) was about 10% below the lower hysteretic point for the 13.7 nm film. A self-consistent correction on the location of the critical end point could be attempted, but would not significantly change the resultant value for K_1/M.

Finally, a value for the second important anisotropy constant can be determined by recalling the original definition for κ, thus

$$K_u/M=\kappa(K_1/M) . \tag{11}$$

Experimental results for K_1/M and K_u/M using the above procedure are shown in Fig. 4.

A fit of the angular dependence of the resonance field using the FMR technique, in contrast to our method, gives two equations involving linear combinations of K_1/M, K_u/M, and K_u'/M. Typically, one must assume

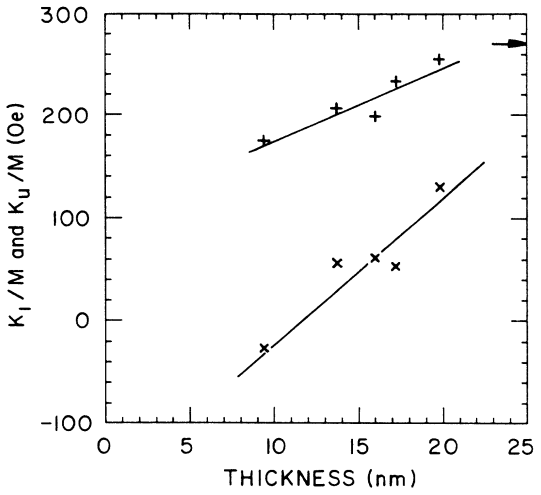

FIG. 4. The values of K_1/M (+) and K_U/M (×) as a function of thickness for the five Fe films studied. The value of K_1/M for bulk iron is marked with an arrow. The lines are drawn as guides to the eye.

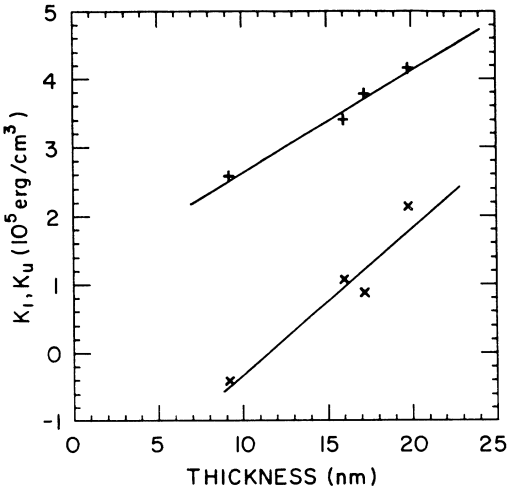

FIG. 5. A plot of K_1 and K_U as a function of thickness using the thickness dependence of M taken from Ref. 27. The lines are drawn as guides to the eye.

that K_1 and M are the same for bulk Fe and solve for the uniaxial constants. In analyzing the MRPT diagram no such assumption is necessary.

Absolute values for the anisotropy constants can be determined if the magnitude of the saturation magnetization is known for each film. SQUID magnetometer studies[2] have shown that this quantity is thickness dependent. A good estimate of M can be obtained by using the extraordinary Hall effect (EHE) (Ref. 19) to determine the field at which M is pulled completely out of the plane of the film. This field is equal to $4\pi M$ if there is no perpendicular anisotropy ($K_n=0$). The EHE data were taken at 4 K but the expected difference between the magnetization at 4 K and at room temperature is well within the experimental error. A plot of K_1 and K_u versus thickness using the EHE results to determine M (the 13.7 nm film was not patterned to enable EHE measurements) is shown in Fig. 5.

A thickness dependence of K_1 has been previously observed in torque magnetometer studies of the single crystal Ni/NaCl system.[31] The in-plane strain was determined from x-ray diffraction data and used to predict the shift in K_1 using five constant magnetostriction data. When the Ni film was floated free of the substrate, the shift in K_1 relative to bulk (ΔK_1) vanished.

If we assume the Fe lattice is strained by the lattice mismatch factor of -1.36% parallel to the interface, then we can determine the complete strain state of the film relative to the crystal axes. Using the five constant magnetostriction data of Bozorth and Hamming,[32] the predicted shift in K_1 due to magnetostriction is $\Delta K_1=0.88\times10^5$ erg/cm^3. This result is the right order of magnitude but the wrong sign to explain the observed shift in K_1. However, this calculation must be viewed with caution since it involves the magnetostriction constants h_3 and h_4 which are extremely difficult to accurately measure and typically have large experimental errors. Unfortunately, we are not able to remove the Fe films from the substrates to check if K_1 shifts back to its bulk value. However, the fact that K_1 varies smoothly with thickness indicates that the explanation is consistent with an origin of magnetostriction arising from a thickness dependent strain.

The variation of K_u with thickness has also been attributed to strain and has been modeled using two constant magnetostriction data by Prinz *et al.*[9] The surprising result, however, is that one would expect K_u to be zero when K_1 was equivalent to that of bulk iron. The reason for this is that since K_1 is sensitive to strain its deviations from the bulk value are a measure of the strain in the sample. Since the value of K_u is zero in bulk iron, then when the measured K_1 equals that of bulk iron, K_u should be zero. As seen in Fig. 5, K_u is monotonically increasing over the entire range of thicknesses investigated and shows no indication of going to zero. We are currently investigating this question with a series of thicker films.

B. Hysteresis

In a previous publication,[10] it was speculated that the hysteresis observed in FMR and magnetization data could be explained by pinning of domain walls by defects arising from either strain relaxing dislocations or the presence of interdiffused Ga or As near the Fe/GaAs interface.[33] Also, line defects or steps not eliminated by the substrate pretreatment have also been noticed in some of the samples. In the present experiments, some of these steps were sufficiently large to disrupt the electrical continuity of the Hall bar samples. Based on the present experimental results, consistent with the above conjecture, we will argue that domain-wall pinning, and not fluctuation-induced hopping over an energy barrier, is the likely source of the observed hysteresis.

It is interesting to calculate the spinodal lines associated with the disappearance of the metastable minima of the energy density corresponding to "superheating" and "supercooling" in a thermal phase transition. These lines are again dependent on the anisotropy constants through the ratio κ. For an applied field along the [110] direction these spinodal points can be calculated explicitly as a function of κ. Following the notation of Arrott *et al.*,[34] we will define h_{p1} as the reduced field where the metastable minimum nearest to the easy [001] direction vanishes as the reduced field is increased. Similarly, the reduced field at which the metastable minimum nearest to the [110] direction disappears as the field is reduced will be called h_{p2}. The results of the calculation for these two points give

$$h_{p1}=(4\sqrt{2}/9)(1+\kappa)^{3/2} \tag{12}$$

and

$$h_{p2}=2\kappa-1\ . \tag{13}$$

It can be verified that the inequality $h_{p1}\geq h_p\geq h_{p2}$ is valid for all allowed values of κ. As before, for applied field directions other than along the [110] direction, the problem becomes impossible to solve analytically. Again solving the resulting system of nonlinear equations numerically we can generate a picture of the spinodal boundaries for given values of the anisotropy constants. The results of this calculation for the 20 nm film is shown in Fig. 6, where the numerical results have been scaled to the experimental data at the critical end point. Of course, at the critical end point ($\theta_H=\theta_{Hc}$), it must be true that $h_1=h_2=h_c$, that is, the spinodal lines must converge at this point. Clearly the hysteresis cannot be explained by the disappearance of the metastable minimum as the field is swept up and down. Also, a point to note is that no

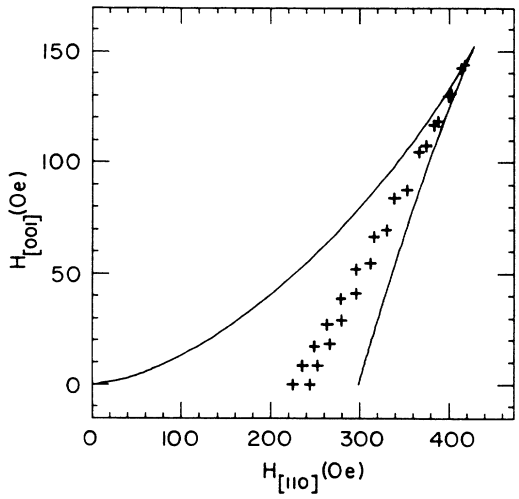

FIG. 6. The calculated phase diagram for a 20-nm film, fitted to the position of the critical end point. The spinodal lines corresponding to the disappearance of the metastable minima are also shown along with the experimental hysteresis data. Note that the experimental points are very different from the spinodal curves indicating that the hysteresis is not due to the dynamics of nucleation.

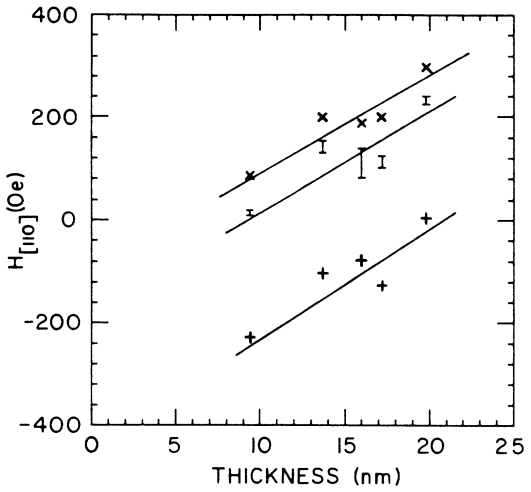

FIG. 7. The hysteresis of each of the films as a function of thickness for the magnetic field in the [110] direction. The × and + points indicate the position of h_{p1} and h_{p2} calculated from Eqs. (12) and (13), respectively. The error bar points indicate the corresponding experimental hysteresis. The lines are a guide for the eye.

time dependence of the hysteresis was observed for sweep rates varying from 5 kOe/min up to 400 kOe/min. Within this range of sweep rates each hysteresis loop was identical to within the resolution of the experiment. In Fig. 7, we show the experimental hysteresis for fields along the [110] direction as well as the points H_{p1} and H_{p2} calculated from Eqs. (12) and (13). Note that for all but the thickest film, a reverse field would have to be applied to eliminate the metastable minimum as the field is swept down if the transitions strictly followed the spinodal lines.

The more likely explanation is that the hysteresis is due to domain-wall pinning. This, as stated previously, is consistent with the large defect density inferred from the

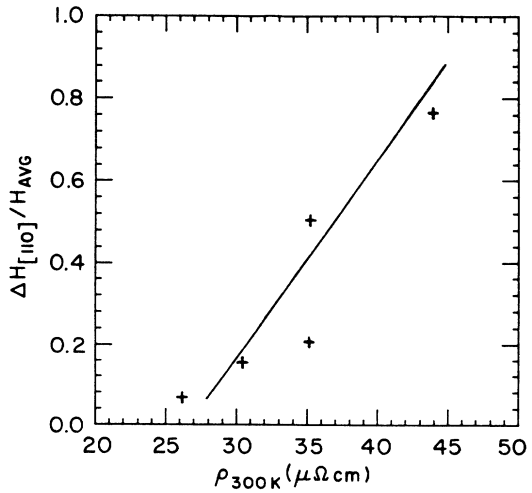

FIG. 8. A comparison of the normalized hysteresis $H_{[110]}/H_{avg}$, where H_{avg} is defined as the midpoint of the hysteresis, to the room temperature resistivity. The line serves as a guide to the eye.

resistivity data. Although it is often stated[35] that the domain walls of a magnetic material are pinned to defects it is unusual to attempt to correlate the coercivity with the resistivity. We have taken this approach in Fig. 8 which a a plot of $\Delta H/H_{\text{avg}}$ along the [110] direction versus ρ. This figure shows that the relative width of the hysteresis increases as the resistivity increases, indicating a correlation with defect density. Although this single figure does not prove directly that the mechanisms causing the increased resistivity in these films are responsible for the increased hysteresis observed, it is suggestive.

VI. CONCLUSIONS

The use of the anisotropic magnetoresistance to probe the first-order MRPT phase diagram has been shown to be a straightforward and powerful method to gain information on the important anisotropy constants that control the magnetic behavior of single crystal cubic ferromagnets with uniaxial anisotropy. The behavior of the lowest order uniaxial anisotropy and the fourth-order cubic anisotropy constants are consistent with previous FMR results. The two advantages of the use of the anisotropic magnetoresistance over FMR are that the experimental requirements are considerably less than for FMR or even torque magnetometry since all that is required is a reasonably good resistance bridge and a modest electromagnet, and the ease of the interpretation of the experimental results.[9]

Another feature of the present research is the thickness dependence of the anisotropy constants as exhibited in Fig. 5. The data for K_1 are inconsistent with the expected strain at the GaAs/Fe interface (the shift in K_1 is of the wrong sign for a compression of the iron films). Also, the variation in the uniaxial anisotropy energy K_u with thickness is interesting since K_1 has nearly reached its bulk iron value in the thickest films, but K_u monotonically increases with increasing thickness even though its bulk value is zero. One might expect if K_u and K_1 have their origins in the strain of the samples that they would both relax to their equilibrium values at similar film thicknesses. The fact that K_u continues to increase with increasing film thickness through the series of samples is therefore strange. In neither case, the sign of the shift in K_1 and the thickness dependence of K_u, is there currently a satisfactory answer.

In addition, interesting hysteresis effects confirming the first-order nature of the transition have been observed. The data clearly indicate that the hysteresis is not what is expected from the calculation of the spinodal lines associated with the disappearance of the metastable minima of the energy density corresponding to "superheating" and "supercooling" in a thermal phase transition. It is much smaller than that calculated and is independent of the sweep rate of the magnetic fields over roughly two orders of magnitude. Although it is difficult to provide a casual relationship for the hysteresis, a correlation with the resistivity has been observed. The resistivity provides a measure of the defect density in the thin films which in turn provides stress fields to pin the magnetic domain walls.[35]

ACKNOWLEDGMENTS

The authors would like to thank Dr. K. Hathaway, Professor L. Berger, and Dr. R. M. White for a number of useful discussions. The research at the University of Minnesota was funded by the U.S. Air Force Office of Scientific Research (AFOSR) Grant Nos. AFOSR-86-0201 and AFOSR-89-0248 and the research at the Naval Research Laboratory was funded by the U.S. Office of Naval Research (ONR). Receipt of the funding is gratefully appreciated.

---

*Present address: Physics Department, Stetson University, P.O. Box 8342, Deland, FL 32720.

[1]A. S. Arrott, B. Heinrich, S. T. Purcell, J. F. Cochran, and K. B. Urquhart, J. Appl. Phys. **61**, 3721 (1987).

[2]T. R. McGuire, J. J. Krebs, and G. A. Prinz, J. Appl. Phys. **55**, 2505 (1984).

[3]S. D. Bader and E. R. Moog, J. Appl. Phys. **61**, 3729 (1987).

[4]J. G. Gay and Roy Richter, J. Appl. Phys. **61**, 3362 (1987).

[5]B. T. Jonker, K.-H. Walker, E. Kisker, G. A. Prinz, and C. Carbone, Phys. Rev. Lett. **57**, 142 (1986).

[6]D. A. Thompson, L. T. Romankiw, and A. F. Mayadas, IEEE Trans. Magn. **MAG-11**, 1039 (1975).

[7]E. Schloemann, R. Tustison, J. Weissman, H. J. Van Hook, and T. Varitimos, J. Appl. Phys. **63**, 3140 (1988).

[8]K. B. Hathaway and G. A. Prinz, Phys. Rev. Lett. **47**, 1761 (1981).

[9]J. J. Krebs, F. J. Rachford, P. Lubitz, and G. A. Prinz, J. Appl. Phys. **53**, 8058 (1982).

[10]F. J. Rachford, G. A. Prinz, J. J. Krebs, and K. B. Hathaway, J. Appl. Phys. **53**, 7966 (1982).

[11]G. A. Prinz, G. T. Rado, and J. J. Krebs, J. Appl. Phys. **53**, 2087 (1982).

[12]G. A. Prinz and J. J. Krebs, Appl. Phys. Lett. **39**, 397 (1981).

[13]D. Mukamel, M. E. Fisher, and E. Domany, Phys. Rev. Lett. **37**, 565 (1976).

[14]J. Cullen and E. Callen, Phys. Rev. B **30**, 181 (1984).

[15]B. Barbara, M. F. Rossignol, and P. Bak, J. Phys. C **11**, L183 (1978).

[16]K. P. Belov, A. K. Zvezdin, R. Z. Levitin, A. S. Markosynan, B. V. Mill, A. A. Mukhin, and A. P. Perov, Zh. Eksp. Teor. Fiz. **68**, 1189 (1975) [Sov. Phys.—JETP **41**, 590 (1976)].

[17]K. Honda and S. Kaya, Sci. Rep. Tohoku Univ. **15**, 721 (1926).

[18]S. D. Hanham, B. Heinrich, and A. S. Arrott, J. Appl. Phys. **50**, 2146 (1979).

[19]K. T. Riggs, E. D. Dahlberg, and G. A. Prinz, J. Magn. Magn. Mater. **73**, 46 (1988).

[20]T. R. McGuire and R. I. Potter, IEEE Trans. Magn. **MAG-11**, 1018 (1975).

[21]E. D. Dahlberg, K. T. Riggs, and G. A. Prinz, J. Appl. Phys.

63, 4270 (1988).
[22]F. J. Rachford, M. Rubinstein, and G. A. Prinz, J. Appl. Phys. **63**, 4291 (1988).
[23]D. C. Jiles and D. L. Atherton, J. Appl. Phys. **55**, 2115 (1984).
[24]P. B. Littlewood and P. Chandra, Phys. Rev. Lett. **57**, 2415 (1986).
[25]A. J. Melmed and J. J. Carroll, J. Vac. Sci. Technol. **10**, 164 (1973).
[26]J. Smit, Physica **16**, 612 (1951).
[27]K. T. Riggs, D. K. Lottis, E. D. Dahlberg, and G. A. Prinz (unpublished).
[28]U. Gradmann, J. Korecki, and G. Waller, Appl. Phys. **39A**, 101 (1986).
[29]R. R. Birss, *Symmetry and Magnetism* (North-Holland, Amsterdam, 1964).
[30]E. P. Wohlfarth, in *Ferromagnetic Materials,* edited by E. P. Wohlfarth (North-Holland, Amsterdam, 1980), Vol. 1.
[31]J. F. Freedman, J. Appl. Phys. **33**, 1148S (1962).
[32]R. M. Bozorth and R. W. Hamming, Phys. Rev. **89**, 865 (1953).
[33]M. W. Ruckman, J. J. Joyce, and J. H. Weaver, Phys. Rev. B **33**, 7029 (1986).
[34]S. D. Hanham, B. Heinrich, and A. S. Arrott, J. Appl. Phys. **50**, 2146 (1979).
[35]B. D. Cullity, *Introduction to Magnetic Materials* (Addison-Wesley, Reading, MA, 1972), p. 325.